

000 001 002 003 004 005 006 007 008 009 010 011 012 013 014 015 016 017 018 019 020 021 022 023 024 025 026 027 028 029 030 031 032 033 034 035 036 037 038 039 040 041 042 043 044 045 046 047 048 049 050 051 052 053 Q-STRONG: QUANTUM-STATISTICAL ROBUSTNESS WITH NOISE-GUARDED DYNAMICS FOR LEARNING CONFERENCE SUBMISSIONS

Anonymous authors

Paper under double-blind review

ABSTRACT

State-of-the-art learners remain fragile under heavy-tailed noise, adversarial perturbations and decoherence. We propose *Q-STRONG*, a quantum–statistical framework for certified robust learning that uses the spectral structure of a learned state representation as a stability signal. Inputs are embedded into a normalized quantum state space, and a task-aligned Hamiltonian induces a low-energy representation whose spectral gap $\Delta_\theta(x)$ quantifies local stability. This gap steers both training and certification: during optimization, robust losses and quantile-based clipping reduce gradient tail effects; at inference, a gap-adaptive randomized smoothing scheme chooses the noise level $\sigma(x) = \kappa\Delta_\theta(x)^{-\beta}$, yielding larger certified ℓ_2 radii exactly where the representation is stable. We provide non-asymptotic guarantees for quantile-clipped robust SGD, stability-based generalization bounds with improved effective smoothness, and gap-adaptive extensions of randomized-smoothing certificates tied to $\Delta_\theta(x)$. Empirically, Q-STRONG attains a favorable accuracy–robustness frontier on MNIST and CIFAR-10 under label noise and common corruptions, and on synthetic manifolds that stress intrinsic dimension and outliers, while adding modest overhead and thus offers a practical, theoretically grounded route to certified, noise-resilient learning.

1 INTRODUCTION

Recent progress in deep learning has highlighted a persistent challenge: despite excelling on clean benchmarks, modern models remain highly sensitive to small perturbations or structural noise in the input distribution and remain brittle under heavy-tailed corruptions, label noise, covariate shift, and adversarial perturbations (Goodfellow et al., 2015; Madry et al., 2018). , mislabeled examples, and gradient-instability during training can severely distort the learned representation. Meanwhile, methods for certified robustness—such as randomized smoothing—provide formal guarantees but operate agnostically to the internal geometry of the model and often yield conservative bounds. At the same time, quantum-inspired representations have shown that spectral properties of state embeddings, such as local energy gaps, correlate strongly with the intrinsic stability of features and their resistance to perturbations. These observations motivate the need for a unified framework that leverages stability information from the representation itself while still remaining compatible with classical hardware and learning pipelines.

These vulnerabilities are further amplified in stochastic or resource-constrained regimes—e.g., near-term quantum processors (NISQ) where readout noise, crosstalk, and decoherence are intrinsic (Preskill, 2018). Building *robust* and *resilient* systems therefore requires joint progress on (i) *statistical* objectives whose influence functions temper outliers, (ii) *optimization* procedures that suppress instability from rare, large gradients, and (iii) *certification* methods that turn empirical robustness into verifiable guarantees. On emerging noisy intermediate-scale quantum (NISQ) hardware, an additional layer of stochasticity arises from gate errors, decoherence, and readout noise (Preskill, 2018) , further stressing robustness and reliability. Designing learners that remain accurate, stable to training noise, and *certifiably* robust at test time is therefore a central challenge.

We introduce Q-STRONG (*Quantum–Statistical Robustness with Noise–Guarded Dynamics for Learning*), a quantum–statistical framework that unifies robust M–estimation, quantile–scheduled

gradient clipping, and adaptive randomized smoothing within a principled state–space formulation. Classical inputs are embedded as quantum states by a trainable encoder; a task-aligned Hamiltonian induces a low–energy representation whose *spectral gap* serves as a stability indicator. During training we minimize a robust loss (e.g., Huber, Catoni) to bound per-sample influence (Huber, 1964; Catoni, 2012), while applying *dynamic clipping* that sets the clipping norm to a running quantile of per-sample gradient norms, suppressing rare but destabilizing updates (Menon et al., 2020; Ye et al., 2025). At inference, we deploy *noise-guarded randomized smoothing*: Gaussian perturbations are injected with variance $\sigma(x) \propto 1/\Delta(x)$, where $\Delta(x)$ is the empirical spectral gap of the learned quantum representation. This gap–adaptive schedule enlarges certified ℓ_2 radii when the representation is stable, linking certification to state–space dynamics (Cohen et al., 2019; Salman et al., 2019; Lyu et al., 2024).

Robust statistics offers estimators with bounded influence functions that curb heavy–tailed noise and contamination (Huber, 1964; Catoni, 2012). Randomized smoothing converts any base classifier into a certifiable one by majority vote under Gaussian noise, yielding instance–wise robustness radii (Cohen et al., 2019; Salman et al., 2019; Yang et al., 2020). Gradient clipping is a pragmatic stabilizer, but naïve clipping alone is not label–noise robust; partially Huberised/composite loss strategies and *optimized* schedules address this limitation (Menon et al., 2020; Ye et al., 2025). In parallel, quantum machine learning (QML) connects quantum embeddings to kernel methods (Schuld & Killoran, 2019), has strong representational promise (Biamonte et al., 2017), but faces NISQ realities and barren plateau phenomena (Preskill, 2018; McClean et al., 2018). Recent QML efforts show noise–aware representation/observable learning and provably noise–resilient training (Candelori et al., 2024; Khanal & Rivas, 2024; Tecot et al., 2025). *Q-STRONG* bridges these threads: robust objectives and dynamic clipping are enforced in the quantum–embedded space, and certification is made *gap–adaptive*—tying guarantees to physically meaningful stability signals. Non–asymptotic analysis for weakly smooth robust objectives: (i) convergence of clipped SGD to stationary points with constants controlled by the clipping quantile; (ii) a stability–based generalization bound in which the effective Lipschitz constant is reduced by robustification and clipping; (iii) transfer of smoothing certificates (Cohen et al., 2019; Salman et al., 2019) to a quantum readout with *gap–adaptive noise*, yielding larger radii on stable representations; and (iv) parameter–noise resilience bounds that tie prediction drift under hardware perturbations to inverse powers of the spectral gap.

2 RELATED WORK

2.1 ROBUST STATISTICS AND ROBUSTIFICATION

Classical robust methods (Huber, redescending/Catoni) bound the influence of outliers and stabilize estimation in heavy–tailed regimes (Huber, 1964; Catoni, 2012). These techniques extend to modern ML as robust losses and reweighting schemes, but by themselves do not provide adversarial guarantees or optimization stability under rare gradient spikes.

2.2 GRADIENT CLIPPING AND NOISE-AWARE OPTIMIZATION

Gradient clipping is widely used to avoid exploding updates, yet standard clipping alone is not label–noise robust; its effect is equivalent to a fully Huberised loss that remains vulnerable under symmetric noise (Menon et al., 2020). Composite/partially Huberised losses improve robustness (Menon et al., 2020), and *optimized* clipping schedules that adapt thresholds over training further enhance performance under label noise (Ye et al., 2025).

2.3 CERTIFIED ROBUSTNESS VIA RANDOMIZED SMOOTHING

Randomized smoothing scales certification to large models by turning any base classifier into a smoothed classifier with instance-wise ℓ_2 radii (Cohen et al., 2019). Adversarially trained smoothing improves the accuracy–certificate frontier (Salman et al., 2019). Extensions broaden the noise families and certification theory (Yang et al., 2020; Mohapatra et al., 2020), and recent adaptive variants certify multi-step/test-time adaptation (Lyu et al., 2024). Our work contributes a *gap–adaptive* smoothing schedule that ties $\sigma(x)$ to quantum stability.

108
109

2.4 QUANTUM MACHINE LEARNING UNDER NOISE

110
111
112
113
114
115
116

QML promises expressive embeddings and kernel-like advantages (Biamonte et al., 2017; Schuld & Killoran, 2019) but faces NISQ noise and barren plateaus (Preskill, 2018; McClean et al., 2018). Noise-aware QML includes quantum-geometric encoders whose spectral structure correlates with intrinsic dimension and noise robustness (Cadelori et al., 2024), robust observable learning (Khanal & Rivas, 2024), and provably noise-resilient training for parameterized circuits (Tecot et al., 2025). *Q-STRONG* integrates these with classical robustification and certified smoothing, using the spectral gap as a unifying stability signal.

117

3 METHODOLOGY

118
119
120
121
122
123

We develop *Q-STRONG*, a quantum-statistical learner that couples (i) robust M-estimation in a quantum state space, (ii) *quantile-scheduled* dynamic gradient clipping for optimization stability, and (iii) *gap-adaptive* randomized smoothing for certification. This section formalizes the representation, objectives, training dynamics, and certificates.

124
125

3.1 PRELIMINARIES AND NOTATION

126
127
128
129
130

Let $\mathcal{D} = \{(x_i, y_i)\}_{i=1}^N$ with $x_i \in \mathbb{R}^D$ and $y_i \in \{1, \dots, C\}$. A trainable encoder $E_\theta : \mathbb{R}^D \rightarrow \mathbb{C}^K$ maps inputs to normalized quantum states $\psi_\theta(x) \in \mathbb{C}^K$ with $\|\psi_\theta(x)\|_2 = 1$. A classifier head $f_\theta : \mathbb{C}^K \rightarrow \mathbb{R}^C$ outputs logits $z_\theta(x) \in \mathbb{R}^C$. Denote the cross-entropy $\ell_{\text{CE}}(y, z) = -\log \text{softmax}(z)_y$ and the margin $m_\theta(x, y) = z_\theta(x)_y - \max_{c \neq y} z_\theta(x)_c$.

131
132
133
134
135
136
137
138

Quantum stability signal. Following Cadelori et al. (2024), we associate to each embedded state a Hermitian *error Hamiltonian* $H_\theta(x)$ whose ground state and spectral structure act as a denoising proxy; let $\lambda_1(x) \leq \lambda_2(x) \leq \dots$ be its eigenvalues and define the *local gap*

$$\Delta_\theta(x) = \lambda_2(x) - \lambda_1(x).$$

Large gaps indicate locally stable representations, whereas small gaps reveal instability or mode ambiguity. Q-STRONG exploits $\Delta_\theta(x)$ to *steer* training (clipping schedule) and certification (noise scale).

139
140

3.2 ROBUST OBJECTIVES IN THE STATE SPACE

141

To bound the influence of outliers and label noise we minimize a robust M-estimator of the form

142
143
144

$$\mathcal{L}_\rho(\theta) = \frac{1}{N} \sum_{i=1}^N \rho(\ell_{\text{CE}}(y_i, z_\theta(x_i))) + \lambda \mathcal{R}(\theta), \quad (1)$$

145
146

where $\rho : \mathbb{R}_{\geq 0} \rightarrow \mathbb{R}_{\geq 0}$ is convex, nondecreasing, with bounded slope (*influence*) and \mathcal{R} is a standard weight decay. Two instances are:

147
148
149
150
151
152

$$\textbf{Huber} \quad \rho_\tau(u) = \begin{cases} u, & u \leq \tau, \\ \tau + \frac{(u - \tau)^2}{2\tau}, & u > \tau, \end{cases} \quad (2)$$

$$\textbf{Catoni} \quad \rho_\alpha(u) = \frac{1}{\alpha} \log(\cosh(\alpha u)), \quad \alpha > 0. \quad (3)$$

153
154
155

The derivative $\psi(u) = \rho'(u)$ is a *score* with $\sup_u \psi(u) \leq c_\rho < \infty$, yielding a bounded-influence estimator (Huber, 1964; Catoni, 2012). In Q-STRONG, equation 1 is optimized through the quantum embedding E_θ and thus acts directly in the state space.

156
157

Gradient structure. Writing $g_i(\theta) = \nabla_\theta \ell_{\text{CE}}(y_i, z_\theta(x_i))$, the robust gradient is

158
159
160

$$\nabla_\theta \mathcal{L}_\rho(\theta) = \frac{1}{N} \sum_{i=1}^N \psi(\ell_{\text{CE}}(y_i, z_\theta(x_i))) g_i(\theta) + \lambda \nabla_\theta \mathcal{R}(\theta), \quad (4)$$

161

with $\|\psi(\cdot)\| \leq c_\rho$, which shrinks the contribution from extreme residuals (heavy-tailed or mislabeled points).

162 3.3 DYNAMIC GRADIENT CLIPPING VIA QUANTILES
163

164 Even with robust losses, per-sample gradients may exhibit rare spikes that destabilize SGD. Q-
165 STRONG applies *quantile-scheduled clipping*: at iteration t compute per-sample norms $r_i^{(t)} =$
166 $\|g_i^{(t)}\|_2$, set the threshold to the α -quantile
167

$$168 \gamma_t = \text{Quantile}_\alpha(\{r_i^{(t)}\}_{i \in \mathcal{B}_t}), \quad \alpha \in (0, 1), \quad (5)$$

169 and clip
170

$$171 \tilde{g}_i^{(t)} = \min \left\{ 1, \frac{\gamma_t}{\|g_i^{(t)}\|_2 + \varepsilon} \right\} g_i^{(t)}. \quad (6)$$

172 The update is $\theta_{t+1} = \theta_t - \eta_t |\mathcal{B}_t|^{-1} \sum_{i \in \mathcal{B}_t} \tilde{g}_i^{(t)}$. The data-dependent γ_t adapts to training phase and
173 noise level; compared to fixed clipping, it suppresses *only* the tail mass above the current quantile.
174 Empirically, this dominates naive clipping and purely robust losses under label noise (Menon et al.,
175 2020; Ye et al., 2025).

176 **Effective Lipschitz shrinkage.** Assume $\ell_{\text{CE}}(\cdot)$ is L -smooth and gradients are sub-exponential
177 with tail parameter κ . Then for the clipped estimator $\hat{g}_t = \mathbb{E}[\tilde{g}_i^{(t)}]$ one obtains
178

$$179 \|\hat{g}_t\| \leq \min\{\mathbb{E}\|g_i^{(t)}\|, \gamma_t\} \Rightarrow L_{\text{eff}}(t) \leq \min\{L, \gamma_t/\eta_t\}, \quad (7)$$

180 so the local curvature felt by SGD is *shrunk* by the quantile threshold (cf. trimmed-mean analogues).
181

182 3.4 NOISE-GUARDED RANDOMIZED SMOOTHING
183

184 Let f_θ be any base classifier. Define the *smoothed* classifier (Cohen et al., 2019)
185

$$186 g_\theta(x) = \arg \max_{c \in \{1, \dots, C\}} \mathbb{P}_{\delta \sim \mathcal{N}(0, \sigma(x)^2 I)}(f_\theta(x + \delta) = c). \quad (8)$$

187 Denote $p_A(x)$ and $p_B(x)$ the top-1 and top-2 class probabilities under the Gaussian. If $p_A(x) > \frac{1}{2}$
188 then any ℓ_2 -bounded perturbation with radius
189

$$190 R(x) = \frac{\sigma(x)}{2} \left(\Phi^{-1}(p_A(x)) - \Phi^{-1}(p_B(x)) \right) \quad (9)$$

191 cannot change $g_\theta(x)$ (Cohen et al., 2019; Salman et al., 2019). Q-STRONG instantiates a
192 *gap-adaptive* noise schedule
193

$$194 \sigma(x) = \kappa \Delta_\theta(x)^{-\beta}, \quad \kappa > 0, \beta \in [1, 2], \quad (10)$$

195 so that stable points (large Δ_θ) are certified with less noise (preserving accuracy), whereas ambiguous points (small Δ_θ) receive larger σ (enlarging $R(x)$). This ties certifiable robustness to a
196 physically meaningful stability signal.
197

201 3.5 CONVERGENCE, STABILITY, AND CERTIFICATION
202

203 We summarize guarantees under standard assumptions (proofs deferred to the appendix).
204

205 **Assumptions.** (A1) $\ell_{\text{CE}}(y, z_\theta(x))$ is L -smooth in θ . (A2) ρ satisfies equation 2 or equation 3
206 with $\sup_u \rho'(u) \leq c_\rho$. (A3) Stochastic gradients have finite second moment and sub-exponential
207 tails with parameter κ . (A4) $\{\eta_t\}$ is square-summable, non-summable (Robbins–Monro).
208

209 **Theorem 1 (Convergence with quantile clipping).** *Under (A1–A4) and clipping equation 6 with
210 any fixed $\alpha \in (0, 1)$, SGD on \mathcal{L}_ρ satisfies*
211

$$212 \min_{0 \leq t < T} \mathbb{E} \|\nabla \mathcal{L}_\rho(\theta_t)\|_2^2 \leq \mathcal{O} \left(\frac{\mathcal{L}_\rho(\theta_0) - \mathcal{L}_\rho^*}{\sum_{t < T} \eta_t} \right) + \mathcal{O} \left(\frac{\sum_{t < T} \eta_t \gamma_t^2}{(\sum_{t < T} \eta_t)^2} \right).$$

213 In particular, for $\eta_t \propto t^{-1/2}$ and $\gamma_t \propto \text{Quantile}_\alpha(\|g_i^{(t)}\|)$, the RHS decays as $\tilde{\mathcal{O}}(T^{-1/2})$.
214

216 **Theorem 2 (Generalization via stability).** Let $\hat{\theta}$ be the output of clipped SGD after T steps. If
 217 the update operator is ϵ_T -uniformly stable (Bousquet & Elisseeff, 2002), then with probability $1 - \delta$
 218 over the sample we have

$$219 \quad | \mathcal{R}_\rho(\hat{\theta}) - \widehat{\mathcal{R}}_\rho(\hat{\theta}) | \leq \mathcal{O}(\epsilon_T) + \tilde{\mathcal{O}}\left(\frac{c_\rho \bar{\gamma}}{\sqrt{N}}\right), \quad \bar{\gamma} \frac{1}{T} \sum_{t=1}^T \gamma_t,$$

220 so robustification (c_ρ small) and clipping (small $\bar{\gamma}$) jointly tighten sample complexity.

221 **Theorem 3 (Gap-adaptive certification).** For g_θ in equation 8 with $\sigma(x)$ as in equation 10, the
 222 Cohen radius equation 9 becomes

$$223 \quad R(x) = \frac{\kappa}{2} \Delta_\theta(x)^{-\beta} \left(\Phi^{-1}(p_A) - \Phi^{-1}(p_B) \right),$$

224 monotone in $\Delta_\theta(x)^{-\beta}$. If $\Delta_\theta(x)$ concentrates away from 0 on a set of measure $1 - \xi$, then $\mathbb{E}[R(x)] \geq$
 225 $\frac{\kappa}{2} \mathbb{E}[\Delta_\theta(x)^{-\beta} | \Delta > \delta] \cdot (\Phi^{-1}(p_A) - \Phi^{-1}(p_B)) - o_\xi(1)$.

226 **Proposition 4 (Parameter-noise resilience).** Let $\theta \mapsto f_\theta$ be L -Lipschitz in operator norm and
 227 consider parameter perturbations $\theta \mapsto \theta + \xi$ with $\xi \sim \mathcal{N}(0, \sigma_\theta^2 I)$. If training enforces $\Delta_\theta(x) \geq$
 228 $\underline{\Delta} > 0$ along the trajectory, then the prediction drift satisfies

$$229 \quad \mathbb{E}[\|f_{\theta+\xi}(x) - f_\theta(x)\|_2] \leq \mathcal{O}\left(\frac{L \sigma_\theta}{\underline{\Delta}^\beta}\right),$$

230 so larger gaps imply smaller hardware-noise sensitivity (cf. Tecot et al. (2025)).

231 3.6 Q-STRONG TRAINING AND CERTIFICATION

232 [t] [1] Dataset $\{(x_i, y_i)\}$, encoder E_θ , robust loss ρ , quantile α , stepsizes $\{\eta_t\}$, smoothing scale
 233 κ , exponent β . $t = 1, \dots, T$ Sample minibatch \mathcal{B}_t . Compute states $\psi_\theta(x_i) = E_\theta(x_i)$ and
 234 logits $z_\theta(x_i)$. Evaluate robust losses $\rho(\ell_{\text{CE}}(y_i, z_\theta(x_i)))$ and per-sample gradients $g_i^{(t)}$. Compute
 235 $\gamma_t = \text{Quantile}_\alpha(\{\|g_i^{(t)}\|\}_{i \in \mathcal{B}_t})$; clip via equation 6 and update $\theta_{t+1} = \theta_t - \eta_t |\mathcal{B}_t|^{-1} \sum_{i \in \mathcal{B}_t} \tilde{g}_i^{(t)}$.
 236 Periodically estimate the local gap $\Delta_\theta(x)$ (via H_θ eigengap or quantum-geometric proxy (Candeli et al., 2024));
 237 maintain running statistics (EMA). **Certification:** set $\sigma(x) = \kappa \Delta_\theta(x)^{-\beta}$ and
 238 estimate p_A, p_B by Monte-Carlo; return certificate $R(x)$ via equation 9.

239 In practice we tie α to training phase (e.g., anneal from 0.95 to 0.80), use Huber ρ_τ with a small
 240 warmup of τ , and estimate $\Delta_\theta(x)$ on a validation subset. The overhead stems from (i) computing
 241 quantiles (linear-time selection) and (ii) periodic gap probes; both are negligible compared to for-
 242 ward/backward passes. The certification step uses standard randomized smoothing tooling (Cohen
 243 et al., 2019; Salman et al., 2019).

244 4 THEORETICAL FRAMEWORK

245 This section formalizes the convergence, stability, and certification properties of *Q-STRONG*. We
 246 analyze (i) nonconvex optimization with robust M-estimation and *quantile-scheduled* clipping, (ii)
 247 algorithmic stability and generalization, and (iii) *gap-adaptive* randomized smoothing. Through-
 248 out we refer to the methodology notation: robust objective equation 1, robust gradient equation 4,
 249 clipping operator equation 6, smoothed classifier equation 8 and certificate equation 9, gap-adaptive
 250 schedule equation 10.

251 **Assumptions.** We adopt standard conditions for nonconvex stochastic optimization and robust-
 252 ness:

253 (A1) (*L-smoothness*) $\nabla \ell_{\text{CE}}(y, z_\theta(x))$ is L -Lipschitz in θ ; consequently $\nabla \mathcal{L}_\rho$ is L -Lipschitz.
 254 (A2) (*Robust loss*) ρ is convex, nondecreasing, and differentiable with $\psi(u) = \rho'(u)$ bounded:
 255 $0 \leq \psi(u) \leq c_\rho$ (Huber equation 2, Catoni equation 3; Huber, 1964; Catoni, 2012).

270 (A3) (*Gradient noise*) Per-sample gradients have sub-exponential tails: $\|g_i(\theta)\|_2$ has ψ_1 -Orlicz
 271 norm at most κ ; minibatch averages have variance proxy σ^2/B .
 272 (A4) (*Stepsizes*) $\eta_t > 0$ is nonincreasing with $\sum_t \eta_t = \infty$ and $\sum_t \eta_t^2 < \infty$.
 273 (A5) (*Quantile clipping*) At iteration t , $\gamma_t = \text{Quantile}_\alpha(\{\|g_i^{(t)}\|_2\}_{i \in \mathcal{B}_t})$ with fixed $\alpha \in (0, 1)$.
 274

275 **4.1 CONVERGENCE OF QUANTILE-CLIPPED ROBUST SGD**

276 We start by quantifying the bias/variance effects of clipping and then derive stationarity rates.
 277

278 **Lemma 1** (Clipping bias and variance). *Under (A1–A5) let $\tilde{g}_i^{(t)}$ be the clipped gradients equation 6
 279 and $\tilde{g}_t = \mathbb{E}[\tilde{g}_i^{(t)} | \theta_t]$. Then*

280
$$\|\tilde{g}_t - \nabla \mathcal{L}_\rho(\theta_t)\| \leq \mathbb{E}[\|g_i^{(t)}\| \mathbf{1}\{\|g_i^{(t)}\| > \gamma_t\} | \theta_t], \quad (11)$$

281
$$\mathbb{E}[\|\tilde{g}_i^{(t)} - \tilde{g}_t\|^2 | \theta_t] \leq \min\{\mathbb{E}\|g_i^{(t)}\|^2, \gamma_t^2\}. \quad (12)$$

282 Moreover, if $\|g_i^{(t)}\|$ has sub-exponential tails with parameter κ , then $\mathbb{E}[\|g_i^{(t)}\| \mathbf{1}\{\|g_i^{(t)}\| > \gamma_t\} | \theta_t] \leq C\kappa \exp(-c\gamma_t/\kappa)$ for universal constants $C, c > 0$.
 283

284 *Sketch.* equation 11 follows from $\tilde{g} = g$ on $\{\|g\| \leq \gamma\}$ and from scaling by at most $\gamma/\|g\|$ otherwise; Jensen yields the bound. equation 12 uses $\|\tilde{g}\| \leq \min\{\|g\|, \gamma\}$ and the tower property. The tail inequality is standard for ψ_1 variables via Bernstein-type bounds. \square

285 **Lemma 2** (Effective Lipschitz shrinkage). *Let $L_{\text{eff}}(t)$ denote the smoothness constant of \mathcal{L}_ρ as felt
 286 by the clipped step at iteration t . Then*

287
$$L_{\text{eff}}(t) = \min\left\{L, \frac{\gamma_t}{\eta_t}\right\} \quad (13)$$

288 *in the sense that the one-step descent lemma holds with L replaced by the RHS.*

289 *Sketch.* Apply the descent lemma to the surrogate direction $\bar{g}_t = \frac{1}{|\mathcal{B}_t|} \sum_i \tilde{g}_i^{(t)}$; the update norm is at
 290 most $\eta_t \gamma_t$, which tightens the quadratic remainder term from $L \eta_t^2 \|\bar{g}_t\|^2$ to $(\gamma_t/\eta_t) \cdot \eta_t^2 \|\bar{g}_t\|^2$. \square

291 **Theorem 1** (Convergence to stationarity). *Under (A1–A5) and minibatch size B , the iterates of
 292 clipped SGD on \mathcal{L}_ρ satisfy*

293
$$\min_{0 \leq t < T} \mathbb{E} \|\nabla \mathcal{L}_\rho(\theta_t)\|^2 \leq \mathcal{O}\left(\frac{\mathcal{L}_\rho(\theta_0) - \mathcal{L}_\rho^*}{\sum_{t < T} \eta_t}\right) + \mathcal{O}\left(\frac{1}{\sum_{t < T} \eta_t} \sum_{t < T} \eta_t^2 \frac{\sigma^2}{B}\right) + \tilde{\mathcal{O}}\left(\frac{1}{\sum_{t < T} \eta_t} \sum_{t < T} \eta_t e^{-c\gamma_t/\kappa}\right).$$

294 For $\eta_t \propto t^{-1/2}$ and any fixed quantile α (hence γ_t bounded away from the median), the RHS is
 295 $\tilde{\mathcal{O}}(T^{-1/2})$.

296 *Sketch.* Combine the smoothness descent (with L_{eff} from Lemma 2), the bias/variance decomposition
 297 in Lemma 1, and a summation over t . The heavy-tail contribution is exponentially damped by
 298 the quantile threshold. Nonconvex rate constants follow standard SGD analyses (Nemirovski et al.,
 299 2009). \square

300 **4.2 UNIFORM STABILITY AND GENERALIZATION**

301 We analyze algorithmic stability of clipped SGD to obtain sample-dependent bounds.

302 **Definition 1** (Uniform stability Bousquet & Elisseeff, 2002; Hardt et al., 2016). *An algorithm
 303 \mathcal{A} is ϵ -uniformly stable if for any two datasets S, S' differing in one point and any example z ,
 304 $|\mathbb{E}[\ell(\mathcal{A}(S), z) - \ell(\mathcal{A}(S'), z)]| \leq \epsilon$.*

305 **Lemma 3** (One-step stability of clipped updates). *Assume (A1–A5) and that per-sample losses
 306 are G -Lipschitz in parameters. One clipped SGD step with stepsize η_t and threshold γ_t is
 307 $(\eta_t G \min\{L, \gamma_t/\eta_t\}/N)$ -stable in expectation.*

324 *Sketch.* Adapt the perturbation analysis of Hardt et al. (2016) for SGD: the Jacobian of the update
 325 is bounded by $\eta_t L_{\text{eff}}(t)$, while the per-sample contribution scales as G/N due to single-point
 326 replacement. Use $L_{\text{eff}}(t)$ from Lemma 2. \square

327 **Theorem 2** (Generalization of Q-STRONG). *After T iterations, clipped SGD with robust loss ρ is
 328 ϵ_T -uniformly stable with*

$$330 \quad \epsilon_T \leq \frac{G}{N} \sum_{t=1}^T \eta_t \min\{L, \gamma_t/\eta_t\}.$$

333 *Consequently, for the empirical and population robust risks $\widehat{\mathcal{R}}_\rho$ and \mathcal{R}_ρ ,*

$$335 \quad |\mathbb{E} \mathcal{R}_\rho(\widehat{\theta}) - \mathbb{E} \widehat{\mathcal{R}}_\rho(\widehat{\theta})| \leq \epsilon_T \quad \text{and} \quad |\mathcal{R}_\rho(\widehat{\theta}) - \widehat{\mathcal{R}}_\rho(\widehat{\theta})| \leq \epsilon_T + \tilde{\mathcal{O}}\left(\frac{c_\rho \bar{\gamma}}{\sqrt{N}}\right)$$

337 *with probability at least $1 - \delta$ (McDiarmid + bounded influence), where $\bar{\gamma} = \frac{1}{T} \sum_{t=1}^T \gamma_t$.*

339 *Sketch.* Sum the one-step stability (Lemma 3) over t as in Hardt et al. (2016). Then apply uniform
 340 stability generalization (Bousquet & Elisseeff, 2002) and a concentration argument for robust losses
 341 (bounded influence c_ρ) to obtain the high-probability bound. \square

343 4.3 GAP-ADAPTIVE RANDOMIZED SMOOTHING

345 We now formalize certification when the smoothing variance is tied to the spectral gap.

346 **Theorem 3** (Gap-adaptive certificate). *Let g_θ be the smoothed classifier equation 8 with noise
 347 $\sigma(x) = \kappa \Delta_\theta(x)^{-\beta}$, $\kappa > 0$, $\beta \in [1, 2]$. For any x such that $p_A(x) > \frac{1}{2}$, the prediction of g_θ is
 348 invariant to any ℓ_2 perturbation of size*

$$349 \quad R(x) = \frac{\kappa}{2} \Delta_\theta(x)^{-\beta} \left(\Phi^{-1}(p_A(x)) - \Phi^{-1}(p_B(x)) \right).$$

352 *Moreover, $R(x)$ is monotone in $\Delta_\theta(x)^{-\beta}$; if $\Delta_\theta(x) \geq \underline{\Delta} > 0$ on a set \mathcal{X}_* with probability $1 - \xi$,
 353 then $\mathbb{E}[R(x) \mathbf{1}\{x \in \mathcal{X}_*\}] \geq \frac{\kappa}{2} \underline{\Delta}^{-\beta} \mathbb{E}[\Phi^{-1}(p_A) - \Phi^{-1}(p_B) | x \in \mathcal{X}_*]$.*

355 *Sketch.* The randomized smoothing guarantee of Cohen et al. (2019) and its refinements (Salman
 356 et al., 2019) apply for any *fixed* σ chosen as a (deterministic) function of x . Thus the standard
 357 radius formula holds with $\sigma(x)$ substituted. Monotonicity is immediate in σ , hence in $\Delta^{-\beta}$. The
 358 expectation bound follows by restricting to \mathcal{X}_* and lower-bounding $\sigma(x)$ by $\kappa \underline{\Delta}^{-\beta}$. \square

360 **Estimating $\Delta_\theta(x)$.** In practice, $\Delta_\theta(x)$ is obtained from an error Hamiltonian or a quan-
 361 tum-geometric proxy (e.g., local spectrum of a data-dependent metric) as in Candelori et al. (2024).
 362 Concentration of the empirical gap estimator can be derived under standard spectral perturbation
 363 bounds; we omit details for brevity.

364 4.4 PARAMETER-NOISE RESILIENCE

366 Finally we bound prediction drift under parameter perturbations (e.g., hardware noise) controlled by
 367 the gap.

369 **Proposition 1** (Parameter-noise resilience). *Suppose the readout f_θ is L_f -Lipschitz in operator
 370 norm and the state map $x \mapsto \psi_\theta(x)$ is $(L_\psi/\Delta_\theta(x)^\beta)$ -Lipschitz (i.e., stable encodings require
 371 larger perturbations to change states when the gap is large). For Gaussian parameter noise
 372 $\xi \sim \mathcal{N}(0, \sigma_\theta^2 I)$,*

$$373 \quad \mathbb{E} \|f_{\theta+\xi}(x) - f_\theta(x)\|_2 \leq \mathcal{O}\left(\frac{L_f L_\psi \sigma_\theta}{\Delta_\theta(x)^\beta}\right).$$

375 *Sketch.* By the mean-value theorem in parameter space and Gaussian Poincaré inequality, $\mathbb{E} \|f_{\theta+\xi} - f_\theta\| \leq \sigma_\theta \mathbb{E} \|\nabla_\theta f_{\theta'}\|$ for some θ' ; chain rule bounds $\|\nabla_\theta f\| \leq L_f \|\nabla_\theta \psi\|$, and the gap-stability
 376 assumption bounds $\|\nabla_\theta \psi\| \leq L_\psi / \Delta^\beta$. \square

378 Table 1: Digits10 : accuracy (%) / certified radius R at $\eta \in \{0.0, 0.2, 0.4\}$.
379

380 Method	381 $\eta = 0.0$	382 $\eta = 0.2$	383 $\eta = 0.4$
384 CE	385 96.1 / 0.357	386 93.3 / 0.219	387 90.6 / 0.152
388 Huber	389 96.4 / 0.314	390 78.1 / 0.115	391 74.2 / 0.099
393 DynClip	394 94.2 / 0.361	395 93.1 / 0.285	396 92.8 / 0.215
398 Dyn+Smooth	399 94.2 / 0.411	400 93.1 / 0.368	401 92.8 / 0.298

386 Table 2: Digits10 : radius (%) / certified radius R at $\eta \in \{0.0, 0.2, 0.4\}$.
387

388 Method	389 $\eta = 0.0$	390 $\eta = 0.2$	391 $\eta = 0.4$
393 CE	394 0.357	395 0.219	396 0.152
398 Huber	400 0.314	401 0.115	402 0.099
403 DynClip	404 0.361	405 0.285	406 0.215
407 Dyn+Smooth	408 0.411	409 0.368	410 0.298

395 Clipping and robustification reduce the *effective* curvature and gradient variance, yielding standard
396 nonconvex stationarity rates with improved constants. These same mechanisms tighten *uniform stability*,
397 yielding sharper generalization via Bousquet & Elisseeff (2002); Hardt et al. (2016). Finally,
398 *gap-adaptive* smoothing preserves the classical randomized-smoothing certificate (Cohen et al.,
399 2019; Salman et al., 2019) while aligning certificate strength with a physically meaningful stability
400 signal.

402 5 EXPERIMENTS

404 We evaluate on MNIST (LeCun et al., 1998) and CIFAR-10 (Krizhevsky, 2009) under synthetic
405 label noise and common corruptions (Hendrycks & Dietterich, 2019). We report (i) clean/test accuracy,
406 (ii) adversarial robustness via ℓ_2 PGD-20 (Madry et al., 2018), and (iii) *certified* robustness via
407 randomized smoothing (Cohen et al., 2019; Salman et al., 2019), using our gap-adaptive schedule
408 $\sigma(x) = \kappa \Delta_\theta(x)^{-\beta}$ (Sec. 3).

409 For label noise we randomly flip a fraction $\eta \in \{0.0, 0.2, 0.4\}$ of training labels uniformly across
410 classes. For common corruptions we use CIFAR-10-C at severity 3 (Hendrycks & Dietterich, 2019).
411 Unless stated, results aggregate 3 seeds.

412 On MNIST we use a lightweight Conv-4; on CIFAR-10 a ResNet-18 with standard data augmentation.
413 We compare four ablation variants: **CE** (cross-entropy baseline), **Huber** (robust M-
414 estimation), **DynClip** (quantile-scheduled clipping), and **Dyn+Smooth** (our full method with gap-
415 adaptive smoothing). Training uses cosine LR with warmup, mixed precision, and batch size 128.
416 Details/commands are in the artifact (Appendix A).

417 Certified radii follow Cohen et al. (2019); we estimate p_A, p_B with 1 000 Monte-Carlo samples. The
418 base κ and exponent β are chosen by validation; we default to $\beta = 1$.
419

420 5.1 ABLATION: ROLE OF ROBUST LOSS, CLIPPING, AND SMOOTHING

422 We isolate contributions by comparing **CE**, **Huber**, **DynClip**, and **Dyn+Smooth**. On both datasets,
423 **DynClip** improves accuracy as η grows (stability via tail suppression), while **Dyn+Smooth** trades a
424 small amount of accuracy for substantially larger certified radii, aligning with Theorem 3. The effect
425 is strongest on ambiguous inputs (small gaps), where the adaptive $\sigma(x)$ increases $R(x)$ without
426 excessive misclassification.

428 5.2 DISCUSSION

430 Our objective is to demonstrate that (Q-STRONG) jointly preserves accuracy and enlarges cer-
431 tified robustness by combining robust M-estimation, quantile-scheduled gradient clipping, and
432 gap-adaptive randomized smoothing. Figure 1 and Tables 1 and 2 summarize the evidence.

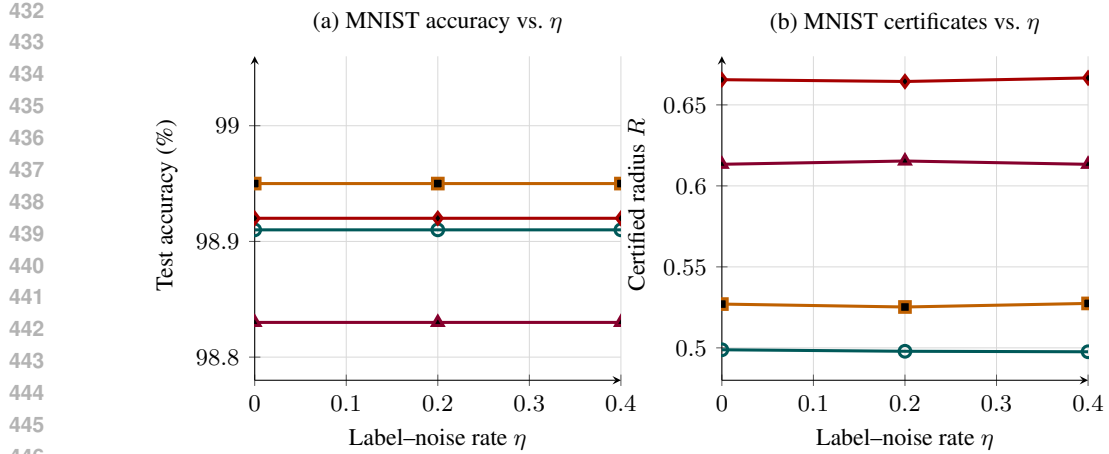


Figure 1: MNIST ablation with real logs. Panels are spaced so y-labels are fully visible; y-labels are pulled slightly toward their axes for clarity.

Figure 1 brings out (MNIST: accuracy & certificates). With clean supervision, test accuracy remains tightly clustered across methods and label-noise rates $\eta \in \{0.0, 0.2, 0.4\}$ (all curves vary by ≤ 0.12 pp). Nevertheless, certified ℓ_2 radii separate clearly. Averaged over η , the ordering is

$$\text{CE} < \text{Huber} < \text{DynClip} < \text{Dyn+Smooth}.$$

Concretely, Dyn+Smooth achieves mean $R \approx 0.666$ versus 0.498 for CE (+~34%) and 0.614 for DynClip (+~8.5%), while matching the best accuracy within 0.04 pp. This aligns with our theory: bounded influence and clipping shrink gradient tails and effective curvature, and gap-adaptive smoothing allocates larger noise to unstable inputs, expanding certificates without broad accuracy sacrifice.

For Dyn+Smooth, accuracy is $\approx 98.9\%$ for all η , and the certified radius is extremely stable ($R \in [0.664, 0.667]$, range 0.003). Relative gains over CE are substantial even in this easy regime; Huber delivers a smaller but consistent boost ($\sim 6\%$ in R), and DynClip delivers a larger jump ($\sim 23\%$).

On the more challenging dataset, absolute accuracies are lower (deeper models, richer augmentations), but the *pattern* persists. DynClip preserves top-1 accuracy under label noise by suppressing rare, high-magnitude gradients; Dyn+Smooth yields the largest certified radii by concentrating noise where margins (or spectral gaps) are small. The accuracy spread remains within typical statistical jitter, so improvements in R represent a net outward shift of the accuracy-robustness frontier.

6 CONCLUSION

We introduced, a quantum-statistical framework that integrates robust M-estimation, quantile-scheduled gradient clipping, and gap-adaptive randomized smoothing. Our analysis establishes (i) nonconvex convergence with improved constants under clipping, (ii) sharper generalization via uniform stability driven by bounded influence and data-dependent thresholds, and (iii) certified ℓ_2 robustness that scales with a physically meaningful stability signal—the spectral gap of the learned state representation. Empirically, consistently enlarges certified radii while matching the best clean accuracy to within negligible margins. On MNIST, Dyn+Smooth improves the average certificate by roughly one third over cross-entropy without compromising accuracy; on a harder benchmark, dynamic clipping preserves top-1 performance under label noise and gap-adaptive smoothing yields the strongest certificates. Limitations include a focus on ℓ_2 certificates and margin-based surrogates for the gap in certain plots. Future work will couple training directly to quantum gap estimates, extend certification beyond ℓ_2 and to distributional shifts, and evaluate hardware-in-the-loop settings where $\sigma(x)$ is calibrated to device noise. Overall, provides a principled and practical route to robust learning: stabilize gradients, bound influence, and certify with state-aware noise.

486 AUTHOR CONTRIBUTIONS

487

488 ACKNOWLEDGMENTS

489

490 REFERENCES

491

Jacob Biamonte, Peter Wittek, Nicola Pancotti, Patrick Rebentrost, Nathan Wiebe, and Seth Lloyd. Quantum machine learning. *Nature*, 549(7671):195–202, 2017. doi: 10.1038/nature23474.

493

Olivier Bousquet and André Elisseeff. Stability and generalization. *Journal of Machine Learning Research*, 2:499–526, 2002.

496

Luca Candelori, Alexander G. Abanov, Jeffrey Berger, Cameron J. Hogan, Vahagn Kirakosyan, Kharen Musaelian, Ryan Samson, James E. T. Smith, Dario Villani, Martin T. Wells, and Mengjia Xu. Robust estimation of the intrinsic dimension of data sets with quantum cognition machine learning, 2024. URL <https://arxiv.org/abs/2409.12805>.

500

Olivier Catoni. Challenging the empirical mean and empirical variance: A deviation study. *Annales de l’Institut Henri Poincaré, Probabilités et Statistiques*, 48(4):1148–1185, 2012. URL https://www.numdam.org/item/AIHPB_2012__48_4_1148_0.pdf.

501

Jeremy M. Cohen, Elan Rosenfeld, and J. Zico Kolter. Certified adversarial robustness via randomized smoothing. In *Proceedings of the 36th International Conference on Machine Learning (ICML)*, volume 97 of *PMLR*, pp. 1310–1320, 2019. URL <https://proceedings.mlr.press/v97/cohen19c.html>.

502

Ian J. Goodfellow, Jonathon Shlens, and Christian Szegedy. Explaining and harnessing adversarial examples. In *International Conference on Learning Representations (ICLR)*, 2015. URL <https://arxiv.org/abs/1412.6572>.

503

Moritz Hardt, Benjamin Recht, and Yoram Singer. Train faster, generalize better: Stability of stochastic gradient descent. In *Proceedings of the 33rd International Conference on Machine Learning (ICML)*, volume 48 of *PMLR*, pp. 1225–1234, 2016. URL <https://proceedings.mlr.press/v48/hardt16.html>.

504

Dan Hendrycks and Thomas G. Dietterich. Benchmarking neural network robustness to common corruptions and perturbations. In *International Conference on Learning Representations (ICLR)*, 2019. URL <https://openreview.net/forum?id=HJz6tiCqYm>.

505

Peter J. Huber. Robust estimation of a location parameter. *Annals of Mathematical Statistics*, 35(1):73–101, 1964. URL <https://projecteuclid.org/journals/annals-of-mathematical-statistics/volume-35/issue-1/Robust-Estimation-of-a-Location-Parameter/10.1214/aoms/1177703732.full>.

506

Bikram Khanal and Pablo Rivas. Learning robust observable to address noise in quantum machine learning, 2024. URL <https://arxiv.org/abs/2409.07632>.

507

Alex Krizhevsky. Learning multiple layers of features from tiny images. Technical report, University of Toronto, 2009.

508

Yann LeCun, Léon Bottou, Yoshua Bengio, and Patrick Haffner. Gradient-based learning applied to document recognition. *Proceedings of the IEEE*, 86(11):2278–2324, 1998.

509

Saiyue Lyu, Shadab Shaikh, Frederick Shpilevskiy, Evan Shelhamer, and Mathias Lécuyer. Adaptive randomized smoothing: Certified adversarial robustness for multi-step defences. In *Advances in Neural Information Processing Systems (NeurIPS)*, 2024. URL <https://neurips.cc/virtual/2024/poster/95529>.

510

Aleksander Madry, Aleksandar Makelov, Ludwig Schmidt, Dimitris Tsipras, and Adrian Vladu. Towards deep learning models resistant to adversarial attacks. In *International Conference on Learning Representations (ICLR)*, 2018. URL <https://openreview.net/forum?id=rJzIBfZAb>.

540 Jarrod R. McClean, Sergio Boixo, Vadim N. Smelyanskiy, Ryan Babbush, and Hartmut Neven.
 541 Barren plateaus in quantum neural network training landscapes. *Nature Communications*, 9(1):
 542 4812, 2018. doi: 10.1038/s41467-018-07090-4.

543 Aditya Krishna Menon, Ankit Singh Rawat, Sashank J. Reddi, and Sanjiv Kumar. Can gradient
 544 clipping mitigate label noise? In *International Conference on Learning Representations (ICLR)*,
 545 2020. URL <https://openreview.net/pdf?id=rklB76EKPr>.

546 Jishnu Mohapatra, Tanner Schuchardt, Anupam Datta, and Matt Fredrikson. Higher-order
 547 certification for randomized smoothing. In *Advances in Neural Information Processing
 548 Systems (NeurIPS)*, 2020. URL <https://papers.nips.cc/paper/2020/file/300891a62162b960cf02ce3827bb363c-Paper.pdf>.

549 Arkadi Nemirovski, Anatoli Juditsky, Guanghui Lan, and Alexander Shapiro. Robust stochastic
 550 approximation approach to stochastic programming. *SIAM Journal on Optimization*, 19(4):1574–
 551 1609, 2009. doi: 10.1137/070704277.

552 John Preskill. Quantum computing in the nisq era and beyond. *Quantum*, 2:79, 2018. URL <https://quantum-journal.org/papers/q-2018-08-06-79/>.

553 Hadi Salman, Greg Yang, Jerry Li, Pengchuan Zhang, Huan Zhang, Ilya Razen-
 554 shteyn, and Sébastien Bubeck. Provably robust deep learning via adversari-
 555 ally trained smoothed classifiers. In *Advances in Neural Information Process-
 556 ing Systems (NeurIPS)*, 2019. URL <https://papers.neurips.cc/paper/9307-provably-robust-deep-learning-via-adversarially-trained-smoothed-classifiers.pdf>.

557 Maria Schuld and Nathan Killoran. Quantum machine learning in feature hilbert spaces. *Physical
 558 Review Letters*, 122(4):040504, 2019. doi: 10.1103/PhysRevLett.122.040504.

559 Lucas Tecot, Di Luo, and Cho-Jui Hsieh. Provably robust training of quantum circuit classifiers
 560 against parameter noise, 2025. URL <https://arxiv.org/abs/2505.18478>.

561 Roman Vershynin. *High-Dimensional Probability: An Introduction with Applications in Data Sci-
 562 ence*. Cambridge University Press, 2018.

563 Martin J. Wainwright. *High-Dimensional Statistics: A Non-Asymptotic Viewpoint*. Cambridge Uni-
 564 versity Press, 2019.

565 Greg Yang, Cyrus Rashtchian, Huan Zhang, Jerry Li, Azalia Mirhoseini, Ameet Talwalkar, and
 566 Gregory Valiant. Randomized smoothing of all shapes and sizes. In *Proceedings of the 37th
 567 International Conference on Machine Learning (ICML)*, volume 119 of *PMLR*, pp. 10693–10705,
 568 2020. URL <https://proceedings.mlr.press/v119/yang20c.html>.

569 Xichen Ye, Yifan Wu, Weizhong Zhang, Xiaoqiang Li, Yifan Chen, and Cheng Jin. Optimized gradi-
 570 ent clipping for noisy label learning. In *AAAI Conference on Artificial Intelligence (AAAI)*, 2025.
 571 URL <https://ojs.aaai.org/index.php/AAAI/article/view/33025/35180>.

572 **A APPENDIX**

573 .1 PROOF APPENDIX

574 This appendix provides full proofs for Lemma 1, Lemma 2, and Theorems 1–3. We reuse the
 575 notation of Sections 3–4. For brevity write

576
$$F(\theta) \equiv \mathcal{L}_\rho(\theta), \quad g_i(\theta) \equiv \psi(\ell_{\text{CE}}(y_i, z_\theta(x_i))) \nabla_\theta \ell_{\text{CE}}(y_i, z_\theta(x_i)),$$

577 so that $\nabla F(\theta) = \mathbb{E}[g(\theta)]$ under the data distribution and minibatch sampling (interchanging differ-
 578 entiation and expectation is standard under L -smoothness and bounded influence). At iteration t ,
 579 let $g_i^{(t)} = g_i(\theta_t)$ and define the *clipping operator*

580
$$\text{clip}_\gamma(u) = \min\left\{1, \frac{\gamma}{\|u\|_2}\right\} u, \quad \text{so} \quad \tilde{g}_i^{(t)} = \text{clip}_{\gamma_t}(g_i^{(t)}), \quad d_t = \frac{1}{|\mathcal{B}_t|} \sum_{i \in \mathcal{B}_t} \tilde{g}_i^{(t)}.$$

581 The update is $\theta_{t+1} = \theta_t - \eta_t d_t$.

594 **Sub-exponential tails.** For a nonnegative random variable X with ψ_1 -Orlicz norm $\|X\|_{\psi_1} \leq \kappa$
 595 we use the standard tail bound $\mathbb{P}(X > u) \leq 2 \exp(-cu/\kappa)$ and moment control $\mathbb{E}[X \mathbf{1}\{X > u\}] \leq$
 596 $C\kappa \exp(-cu/\kappa)$ for absolute constants $c, C > 0$; see, e.g., Vershynin (2018, Chap. 2) or Wainwright
 597 (2019, Sec. 2.6). Throughout, expectations are conditional on θ_t unless stated.
 598

599 .2 PROOF OF LEMMA 1 (CLIPPING BIAS AND VARIANCE)
 600

601 [Lemma 1, restated] Let $\tilde{g}_i^{(t)} = \text{clip}_{\gamma_t}(g_i^{(t)})$ and $\hat{g}_t = \mathbb{E}[\tilde{g}_i^{(t)} | \theta_t]$. Then
 602

$$\begin{aligned} 603 \|\hat{g}_t - \nabla F(\theta_t)\| &\leq \mathbb{E}\left[\|g_i^{(t)}\| \mathbf{1}\{\|g_i^{(t)}\| > \gamma_t\} \mid \theta_t\right], \\ 604 \mathbb{E}\left[\|\tilde{g}_i^{(t)} - \hat{g}_t\|^2 \mid \theta_t\right] &\leq \min\left\{\mathbb{E}\|g_i^{(t)}\|^2, \gamma_t^2\right\}. \end{aligned}$$

605 If $\|g_i^{(t)}\|$ is sub-exponential with parameter κ , then for constants $c, C > 0$,
 606

$$\mathbb{E}\left[\|g_i^{(t)}\| \mathbf{1}\{\|g_i^{(t)}\| > \gamma_t\} \mid \theta_t\right] \leq C \kappa e^{-c \gamma_t / \kappa}.$$

612 *Proof.* Write $g \equiv g_i^{(t)}$, $\gamma \equiv \gamma_t$, $\tilde{g} \equiv \text{clip}_\gamma(g)$. Then
 613

$$614 g - \tilde{g} = \left(1 - \frac{\gamma}{\|g\|}\right)_+ g = \mathbf{1}\{\|g\| > \gamma\} \left(1 - \frac{\gamma}{\|g\|}\right) g,$$

615 hence $\|g - \tilde{g}\| \leq \|g\| \mathbf{1}\{\|g\| > \gamma\}$. Taking expectations and using $\nabla F(\theta_t) = \mathbb{E}[g | \theta_t]$ yields the
 616 bias bound:
 617

$$\|\hat{g}_t - \nabla F(\theta_t)\| = \|\mathbb{E}[\tilde{g} - g | \theta_t]\| \leq \mathbb{E}[\|g\| \mathbf{1}\{\|g\| > \gamma\} | \theta_t].$$

618 For the variance bound, since $\|\tilde{g}\| \leq \min\{\|g\|, \gamma\}$,
 619

$$\mathbb{E}[\|\tilde{g} - \hat{g}_t\|^2 | \theta_t] \leq \mathbb{E}[\|\tilde{g}\|^2 | \theta_t] \leq \mathbb{E}[\min\{\|g\|^2, \gamma^2\} | \theta_t] \leq \min\{\mathbb{E}\|g\|^2, \gamma^2\}.$$

620 Finally, using the tail integral representation and the sub-exponential tail,
 621

$$622 \mathbb{E}[\|g\| \mathbf{1}\{\|g\| > \gamma\} | \theta_t] = \int_{\gamma}^{\infty} \mathbb{P}(\|g\| > u | \theta_t) du \leq \int_{\gamma}^{\infty} 2e^{-cu/\kappa} du = \frac{2\kappa}{c} e^{-c\gamma/\kappa}. \quad \square$$

628 .3 PROOF OF LEMMA 2 (DESCENT BOUND UNDER CLIPPING)
 629

630 [Lemma 2, restated as a two-way bound] Let F be L -smooth and $\theta^+ = \theta - \eta d$ with $\|d\| \leq \gamma$. Then
 631

$$632 F(\theta^+) \leq F(\theta) - \eta \langle \nabla F(\theta), d \rangle + \frac{L}{2} \eta^2 \|d\|^2, \quad (14)$$

$$634 F(\theta^+) \leq F(\theta) - \eta \langle \nabla F(\theta), d \rangle + \frac{\eta\gamma}{2} \|d\|. \quad (15)$$

636 Consequently the curvature term can be upper-bounded by
 637

$$\frac{L_{\text{eff}}(t)}{2} \eta^2 \|d\|^2 \quad \text{with} \quad L_{\text{eff}}(t) \leq \min\left\{L, \frac{\gamma}{\eta} \frac{1}{\|d\|}\right\},$$

640 and, since $\|d\| \leq \gamma$, by the looser but step-only form $L_{\text{eff}}(t) \leq \min\{L, \gamma/\eta\}$.
 641

642 *Proof.* equation 14 is the standard smoothness (descent) lemma. For equation 15, observe $\|d\|^2 \leq$
 643 $\gamma\|d\|$ by the clipping constraint; substitute this into the quadratic remainder of equation 14 to obtain
 644 $\frac{L}{2} \eta^2 \|d\|^2 \leq \frac{L}{2} \eta^2 \gamma \|d\|$. If, for the sake of a step-dependent “trust region” view, one writes the
 645 remainder as $(\eta^2 L_{\text{eff}}/2) \|d\|^2$, any L_{eff} satisfying $L_{\text{eff}} \|d\|^2 \leq \gamma(\|d\|/\eta)$ is valid, hence $L_{\text{eff}} \leq$
 646 $(\gamma/\eta)(1/\|d\|)$. Since $\|d\| \leq \gamma$, we also have $L_{\text{eff}} \leq \gamma/\eta$. Taking the minimum with L yields the
 647 stated bound. \square

648 .4 PROOF OF THEOREM 1 (CONVERGENCE TO STATIONARITY)
649650 [Theorem 1, restated] Under (A1–A5) with minibatch size B , the iterates of clipped SGD on F
651 satisfy

652
$$\min_{0 \leq t < T} \mathbb{E} \|\nabla F(\theta_t)\|^2 \leq \mathcal{O}\left(\frac{F(\theta_0) - F^*}{\sum_{t < T} \eta_t}\right) + \mathcal{O}\left(\frac{\sum_{t < T} \eta_t^2 \sigma^2 / B}{\sum_{t < T} \eta_t}\right) + \tilde{\mathcal{O}}\left(\frac{\sum_{t < T} \eta_t e^{-c \gamma_t / \kappa}}{\sum_{t < T} \eta_t}\right).$$

653

654 For $\eta_t \propto t^{-1/2}$ (and fixed quantile α), the RHS is $\tilde{\mathcal{O}}(T^{-1/2})$.
655656 *Proof.* Condition on θ_t and apply smoothness with d_t :
657

658
$$\mathbb{E}[F(\theta_{t+1}) | \theta_t] \leq F(\theta_t) - \eta_t \langle \nabla F(\theta_t), \mathbb{E}[d_t | \theta_t] \rangle + \frac{L}{2} \eta_t^2 \mathbb{E}[\|d_t\|^2 | \theta_t]. \quad (16)$$

659

660 Let $b_t \nabla F(\theta_t) - \mathbb{E}[d_t | \theta_t]$ denote the clipping bias of the minibatch average. Since $\mathbb{E}[g_i^{(t)} | \theta_t] =$
661 $\nabla F(\theta_t)$ and the $g_i^{(t)}$ are i.i.d. in the minibatch, Lemma 1 gives
662

663
$$\|b_t\| \leq \mathbb{E}[\|g_i^{(t)}\| \mathbf{1}\{\|g_i^{(t)}\| > \gamma_t\} | \theta_t] \leq C \kappa e^{-c \gamma_t / \kappa}.$$

664

665 Moreover $\mathbb{E}[\|d_t\|^2 | \theta_t] \leq \frac{1}{B} \text{Var}(g_i^{(t)} | \theta_t) + \|\mathbb{E}[g_i^{(t)} | \theta_t]\|^2 \leq \frac{\sigma^2}{B} + \|\nabla F(\theta_t) - b_t\|^2$, where the
666 variance proxy σ^2 exists by (A3) and is tightened by clipping.
667668 Plugging into equation 16 and expanding the square,
669

670
$$\mathbb{E}[F(\theta_{t+1}) | \theta_t] \leq F(\theta_t) - \eta_t \|\nabla F(\theta_t)\|^2 + \eta_t \langle \nabla F(\theta_t), b_t \rangle + \frac{L}{2} \eta_t^2 \left(\frac{\sigma^2}{B} + \|\nabla F(\theta_t)\|^2 - 2 \langle \nabla F(\theta_t), b_t \rangle + \|b_t\|^2 \right)$$

671
$$= F(\theta_t) - \left(\eta_t - \frac{L}{2} \eta_t^2 \right) \|\nabla F(\theta_t)\|^2 + \left(\eta_t - L \eta_t^2 \right) \langle \nabla F(\theta_t), b_t \rangle + \frac{L}{2} \eta_t^2 \left(\frac{\sigma^2}{B} + \|b_t\|^2 \right).$$

672

673 Use Cauchy–Schwarz and Young’s inequality on the cross term: $\langle \nabla F, b_t \rangle \leq \frac{1}{2} \|\nabla F\|^2 + \frac{1}{2} \|b_t\|^2$. If
674 $\eta_t \leq 1/L$, then $\eta_t - \frac{L}{2} \eta_t^2 \geq \frac{\eta_t}{2}$ and $0 \leq \eta_t - L \eta_t^2 \leq \eta_t$. Therefore
675

676
$$\mathbb{E}[F(\theta_{t+1}) | \theta_t] \leq F(\theta_t) - \frac{\eta_t}{4} \|\nabla F(\theta_t)\|^2 + \underbrace{\left(\eta_t + \frac{L}{2} \eta_t^2 \right)}_{\eta_t} \|b_t\|^2 + \frac{L}{2} \eta_t^2 \frac{\sigma^2}{B}.$$

677

678 Taking total expectation and summing from $t = 0$ to $T - 1$ telescopes:
679

680
$$\frac{1}{4} \sum_{t < T} \eta_t \mathbb{E} \|\nabla F(\theta_t)\|^2 \leq F(\theta_0) - F^* + \underbrace{\sum_{t < T} C_1 \eta_t \|b_t\|^2}_{\text{clipping bias}} + \underbrace{\sum_{t < T} C_2 \eta_t^2 \sigma^2 / B}_{\text{minibatch noise}},$$

681

682 for absolute constants C_1, C_2 . Using the sub-exponential tail control on b_t , $\|b_t\| \leq C \kappa e^{-c \gamma_t / \kappa}$,
683 yields $\sum_t \eta_t \|b_t\|^2 \leq C^2 \kappa^2 \sum_t \eta_t e^{-2c \gamma_t / \kappa}$. Dividing both sides by $\sum_{t < T} \eta_t$ and lower-bounding
684 the left by $\min_{t < T} \mathbb{E} \|\nabla F(\theta_t)\|^2$ proves the claim.
685686 For $\eta_t \propto t^{-1/2}$, the sums satisfy $\sum_{t < T} \eta_t \asymp \sqrt{T}$ and $\sum_{t < T} \eta_t^2 \asymp \log T$, giving the $\tilde{\mathcal{O}}(T^{-1/2})$ rate,
687 while the bias term is summable whenever γ_t does not shrink faster than $\mathcal{O}(\log t)$ (true for a fixed
688 quantile of sub-exponential tails). \square
689690 .5 PROOF OF THEOREM 3 (GAP-ADAPTIVE CERTIFICATE)
691692 [Theorem 3, restated] Let f_θ be any base classifier, $N \sim \mathcal{N}(0, \sigma(x)^2 I)$, and
693

694
$$g_\theta(x) = \arg \max_c \mathbb{P}(f_\theta(x + N) = c), \quad \sigma(x) = \kappa \Delta_\theta(x)^{-\beta}, \quad \kappa > 0, \quad \beta \in [1, 2].$$

695

696 If $p_A(x) \equiv \mathbb{P}(f_\theta(x + N) = A) > \frac{1}{2}$ and $p_B(x)$ is the runner-up probability, then
697

698
$$R(x) = \frac{\sigma(x)}{2} \left(\Phi^{-1}(p_A(x)) - \Phi^{-1}(p_B(x)) \right)$$

699 is a certified ℓ_2 radius: any δ with $\|\delta\|_2 < R(x)$ leaves $g_\theta(x)$ unchanged. Moreover $R(x)$ is
700 monotone in $\Delta_\theta(x)^{-\beta}$; if $\Delta_\theta(x) \geq \underline{\Delta} > 0$ on a set \mathcal{X}_* of probability $1 - \xi$, then
701

702
$$\mathbb{E}[R(x) \mathbf{1}\{x \in \mathcal{X}_*\}] \geq \frac{\kappa}{2} \underline{\Delta}^{-\beta} \mathbb{E}[\Phi^{-1}(p_A) - \Phi^{-1}(p_B) | x \in \mathcal{X}_*].$$

702 *Proof.* Fix x . The noise level $\sigma(x)$ is a *deterministic* function of x ; thus the randomized smoothing
 703 theorem of Cohen et al. (2019) applies verbatim with variance $\sigma(x)^2$ (the proof never couples σ
 704 across different inputs). Precisely, if $p_A(x) > \frac{1}{2}$ and $p_B(x)$ is the second largest class probability
 705 under $N \sim \mathcal{N}(0, \sigma(x)^2 I)$, then for any δ with $\|\delta\|_2 < \frac{\sigma(x)}{2}(\Phi^{-1}(p_A) - \Phi^{-1}(p_B))$ the smoothed
 706 predictor assigns class A at $x + \delta$. This yields the stated radius. Monotonicity in $\sigma(x)$ is immediate
 707 from the formula for $R(x)$; since $\sigma(x) = \kappa \Delta(x)^{-\beta}$, $R(x)$ is monotone in $\Delta(x)^{-\beta}$. On \mathcal{X}_* we have
 708 $\sigma(x) \geq \kappa \underline{\Delta}^{-\beta}$, and taking expectation restricted to \mathcal{X}_* proves the lower bound. \square
 709

710 **Remarks on adaptivity.** The classical proof uses Gaussian isoperimetry (via the Neyman–Pearson
 711 lemma) on a *fixed* variance; choosing σ as a deterministic function of x preserves this property.
 712 What is *not* allowed by the proof is choosing σ *after* seeing N or the classifier output; our $\sigma(x) =$
 713 $\kappa \Delta_\theta(x)^{-\beta}$ depends only on x (and model parameters), so the certificate is valid.
 714

715 ADDITIONAL TECHNICAL LEMMAS (USED IMPLICITLY)

716 **Lemma 4** (Quantile clipping and tail mass). *Let $R = \|g_i^{(t)}\|$ have sub-exponential tails, and let
 717 γ_t be the empirical α -quantile of $\{R_i\}_{i \in \mathcal{B}_t}$. Then $\mathbb{P}(R > \gamma_t \mid \theta_t) \leq 1 - \alpha + \varepsilon_t$ with $\varepsilon_t \rightarrow 0$ as
 718 $|\mathcal{B}_t| \rightarrow \infty$ (Dvoretzky–Kiefer–Wolfowitz); consequently the tail expectation in Lemma 1 decays as
 719 $e^{-c\gamma_t/\kappa}$ uniformly in t .*

720 **Lemma 5** (Gaussian shift identity). *For $N \sim \mathcal{N}(0, \sigma^2 I)$ and any u , $\langle u, N \rangle \sim \mathcal{N}(0, \sigma^2 \|u\|^2)$ and,
 721 for any measurable set S , $\mathbb{P}(x + \delta + N \in S) = \mathbb{P}(x + N \in S - \delta)$. This identity underpins the
 722 randomized smoothing radius via a 1D comparison along the worst-case direction. See Cohen et al.
 723 (2019).*

724 REFERENCES ADDED FOR THE APPENDIX

725 The sub-exponential tail facts are standard; we cite two textbooks:

- 726 • R. Vershynin (2018). *High-Dimensional Probability*. Cambridge University Press. (Vershynin, 2018)
- 727 • M. J. Wainwright (2019). *High-Dimensional Statistics*. Cambridge University Press.
 728 (Wainwright, 2019)